CONF-800724--57

DOE-ER-03992-409

August 1980

A REVIEW ON DTU-PARTON MODEL FOR HADRON-HADRON AND HADRON-NUCLEUS COLLISIONS

By

Charles B. Chiu

The Center for Particle Theory
THE UNIVERSITY OF TEXAS AT AUSTIN

DISCLAIMER

A REVIEW ON DTU-PARTON MODEL FOR HADRON-HADRON AND HADRON-NUCLEUS COLLISIONS*,**

Charles B. Chiu

Center for Particle Theory, Department of Physics

University of Texas, Austin, Texas 78712

Abstract

The parton picture of color separation of dual string and its subsequent breakup is used to motivate the DTU-parton model for high energy small p_T multiparticle productions in hadron-hadron and hadron-nucleus collisions. A brief survey on phenomenological applications of the model: such as the inclusive spectra for various hh processes and central plateau heights predicted, hA inclusive spectra and the approximate $\overline{\nu}$-universalities is presented.

Madison, Wisconsin

*A talk presented at the XX International Conference on High Energy Physics.

**This work was supported in part by the U.S. Department of Energy.

July 17-23, 1980

A REVIEW ON DTU-PARTON MODEL FOR hh AND hA COLLISIONS*

Charles B. Chiu
Center for Particle Theory, Univeristy of Texas, Austin, Texas

Recently several groups[1-5] have considered small-p_T models, which combine features from both the parton model and the DTU model. We shall refer to them loosely as the DTU-parton model. In this talk, we take a definite point of view to motivate this model, and based on this framework we briefly survey its phenomenological applications to hadron-hadron and hadron-nucleus collisions.

Data indicate that small p_T-multiparticle productions constitute a large fraction of final particles in hadron collisions. Within QCD, these productions are presumably dominated by nonperturbative mechanisms, where confinement plays an important role. A suggestive parton picture is that immediately after hadron collisions, tube-like color-singlet-systems are created. Each tube consists of a 3 and a $\overline{3}$ color charges at its two ends. They are connected by gluon flux.[6,7] Pair productions within the tube break up the tube into a chain of tubelets, or hadrons.

Now if we identify the tube-like systems as the dual strings, it is natural to describe the multiparticle productions by the dual resonance model, or in its "developed form": the DTU model.[8] For illustration, consider first meson-meson (MM) collisions. Here the dominant multiparticle production diagrams contributing to the Pomeron are the two-chain diagrams. Typical examples are illustrated in Fig. 1, where the longitudinal rapidity coordinate y is along the vertical direction. For the MM case, there are altogether four "y-ordered" diagrams. These are the two illustrated and the other two with the 3 and $\overline{3}$ labels interchanged.

Denote the rapidities of the inner boundaries of the two chains by y_1 and y_2. According to DTU, their distribution is given by:

$$\frac{d^2n}{dy_1dy_2} \sim \exp[\alpha y_1 + \alpha_P(y_2 - y_1) + \alpha(Y - y_2)] \sim \frac{1}{\sqrt{-x_1x_2}} , \qquad (1)$$

where we have used $\alpha_P \approx 1$ and $\alpha \approx 0.5$. Note that from the distributions given, the average values: $\langle y_1\rangle = \langle Y - y_2\rangle \approx 2$. So the inner ends are displaced by 2 units from the corresponding kinematic boundaries. Their spectra in plateau approximation are illustrated in Figs. 2a,b. Fig. 2a will be referred to as the 2-displaced-chain (2DC) spectrum, and Fig. 2b the short-long-chain (SLC) spectrum. Note that within the plateau approximation, the two resultant spectra are the same. For the pp case, p may be treated again as a 3(q) and $\overline{3}$(qq) system. Furthermore, DTU favors the diquark to carry most of its parent-hadron momentum.[3] Consequently, the pp case gives predominantly a 2DC spectrum, while the $\overline{p}p$ case, a SLC spectrum.

*Work was supported in part by the U.S. Department of Energy.

The corresponding more realistic DTU spectra are sketched in 2c and 2d, where the spectrum near each end approaches zero like $(1-x)^n$, with x being the magnitude of the Feynman variable defined in the rest frame of the chain. The power n varies for different types of endings. Also n should in general depend on t, where for $a \to cX$, $t = (p_a - p_c)^2$. This very t-dependent power behavior has been confirmed: e.g.[9] in $\pi^{\pm}p \to \pi^0 X$. More specifically, the triple Regge prediction of DTU gives $n = 1 - 2\alpha(t)$, with $\alpha(t)$ being the ρ trajectory. The power behavior extracted from their data compared quite favorably with the ρ trajectory. (See Fig. 3.)

Analyses on inclusive distributions have been reported by Capella et al.[1] and by Cohen-Tannoudji et al.[3] on the following reactions:

$$x=0\to 1 \begin{cases} pp \to \pi_{ch} X, \\ \pi^{\pm}p \to \text{(charge poles)}X, \\ \bar{p}p \to \text{(charge poles)}X,\ \pi^{+}X. \end{cases} ;0.1 \leq x \leq 0.9 \begin{cases} \pi^{\mp}p \to \pi^{\pm}X \\ \pi^{+}p \to \pi^{+}X \text{ (nondiffr.)} \\ K^{+}p \to \pi^{-}X \end{cases}$$

Since only t-integrated data have been considered, the power n at different ends have been treated as constant parameters. In the future, it is worthwhile to determine n as a function t.

For central plateau heights at nonasymptotic energies there is the following regularity[1]: $h_{pp} < h_{\pi p} < h_{\bar{p}p}$. This stems from the fact that: at present energies h_{pp} is a sum of heights of two shoulders (see Fig. 2c), while $h_{\bar{p}p}$ is a sum of two central maxima (see Fig. 2d). The πp case is contributed by both the pp type and the $\bar{p}p$ type. So it falls in between. The energy dependence of these central plateau heights is illustrated in Fig. 4. The pp data is also included for comparison. Notice that the rise of the central plateau is naturally explained here.

In the context of the DTU-parton model, $\bar{p}p$ annihilation process has recently been considered by Sukhatme.[2] DTU predicts that the 3-chain annihilation processes should dominate all annihilation diagrams with its cross section goes like $1/\sqrt{s}$. The energy dependence of $h_{\bar{p}p}$ of annihilation is also illustrated in Fig. 4. Asymptotically the ratio of annihilation to non-annihilation heights approaches 3/2, a reflection of 3-chain versus 2-chain topologies.

Now we turn to hA collisions. Earlier we have assumed that it is the pair production within the tube, which leads to the breakup of the tube. It is plausible that the pair production time τ_0, defined in the rest frame of the pair should be a constant. In fact, in the flux tube model[6] τ_0 can be estimated qualitatively. In particular, the probability of the pair production per unit time per volume has been estimated to be[6]: $P \approx 10^{-3}\ \text{GeV}^4$. So $1/\tau_0 \approx PV$, where the available volume V is approximately $\pi r^2 \tau_0$. Assume $r \sim 1/m_\pi$, we get $1/\tau_0 \sim 0.4$ GeV. Now the time taken for each pair with rapidity y to travel a distance d is $t = d/\tanh y$. This implies that within the spatial interval d, there is a critical rapidity $y_c = \sinh^{-1}(d/\tau_0)$, such that only for $y \leq y_c$, $q\bar{q}$ pairs will have time to be produced. Taking $d \sim 1/m_\pi$ we get $y_c \approx 1.8$. So the upshot is that, consider two consecutive collisions, immediately before the second collision, only pairs up to $y \approx 2$ will be produced.

For a proton projectile, this next collision is expected to be dominated between the energetic tube system N* (the unbroken tube II in Fig. 1a) and the target nucleon. We assume that the spectrum of N*N collision is similar to that of pp collision. This then leads to the spectrum of Fig. 5, where there are two chain-I spectrum and one chain-II spectrum. In general for $\bar{\nu}$ collisions, there would be $\bar{\nu}$ chain-I's and one chain-II. So the ratio

$$R = \langle n \rangle_{hA} / \langle n \rangle_{hh} = (\bar{\nu}+1)/2 \ . \tag{2}$$

For the pA case, Chao et al.[4] showed that the comparison between their model and the available dn/dy pA data are satisfactory. Their comparison: R vs $\bar{\nu}$ for 200 GeV pA data is shown in Fig. 6, where "a" corresponds to having only N*N collisions as the successive collisions. The agreement is satisfactory. The dotted line: "b", is the prediction including also the remaining interactions between the less energetic tube and target nucleons, which have not interacted with N*, the energetic projectile system. The agreement here is even better.

Next we turn to the $\bar{p}$A case (see Fig. 7). Using similar argument as that for the pp case and the approximate relation indicated above: $y_c \sim y_1 \sim 2$, we get e.g. the plateau spectrum of Fig. 8. A comparison with Fig. 5 leads to the statement of $\bar{\nu}$-universality: i.e. for $\bar{\nu}_{pA} = \bar{\nu}_{pA'} = \nu_{MA''}$

$$dn/dy|_{pA} \approx dn/dy|_{pA'} \approx dn/dy|_{MA''} \ . \tag{3}$$

In ref. 5, it has also been shown that the above $\bar{\nu}$ universality condition persists, so long as the inequality $y_c \geqq y_1$ is satisfied. For instance, denote $\Delta = y_c - y_1$, within the same plateau approximation, both pA and $\bar{p}$A' cases lead to

$$R = (\bar{\nu}+1)/2 + \Delta(\bar{\nu}-1)/[2(Y-y_1)] \ . \tag{4}$$

We recall that y_c is related to the pair production rate within the confining flux tube. So the above discussion illustrates how nuclear targets provide a unique arena for confinement related information, not available in hh collisions.

Finally we mention that Capella and Tran[10] have also considered a hA model, assuming that projectile sea quarks also form additional tubes in small-p_T productions. This assumption leads to the asymptotic prediction: $R \sim \bar{\nu}$. However, at present energies, phenomenological predictions of the models of ref. 4 and ref. 10 have been shown to be similar for the pA case.

We thank Rudy Hwa, Uday Sukhatme and Chung-I Tan for stimulating discussions.

REFERENCES

1. Capella et al., Phys. Lett. 81B, 68 (1979); Z. Phys. C3, 329

(1980).
2. Sukhatme, Phys. Rev. Lett. 44, 518 (1980).
3. Cohen-Tannoudji et al., Saclay preprint Dph-T/79-92.
4. Chao et al., Phys. Rev. Lett. 44, 518 (1980).
5. Chiu and Tow, CPT preprint, 1980 (DOE-ER-397), revised.
6. Casher et al., Phys. Rev. D20, 179 (1979); refs. therein.
7. Donoghue, MIT preprint, 1980 (CTP-829).
8. Chan et al, NP B86, 479 (1975); Chew et al, Phys. Rep. 41C, 263 (1978).
9. Caltech-LBL collaboration, Nucl. Phys. B145, 45 (1978).
10. Capella and Tran, Orsay preprint, 1980.

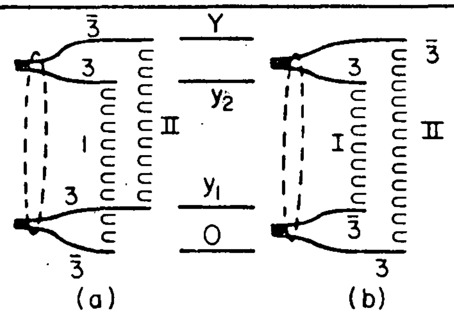

Fig. 1. 2-chain diagrams:
a. 2-displaced chains (2DC)
b. short-long chains (SLC)

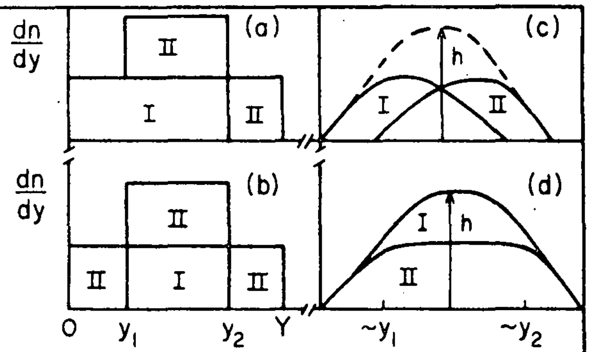

Fig. 2. y-spectra of 2-chain diagrams:
a,c. 2DC spectra
b,d. SLC spectra

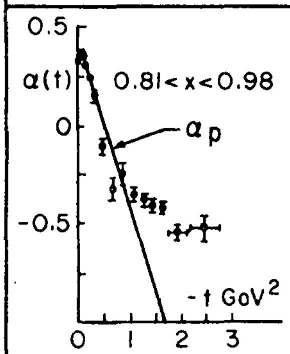

Fig. 3. α extracted from $(1-x)^{1-2\alpha(t)}$

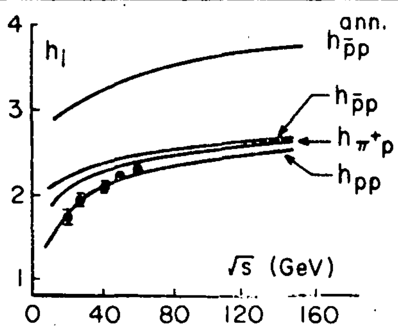

Fig. 4. Energy dependence of central plateaus.

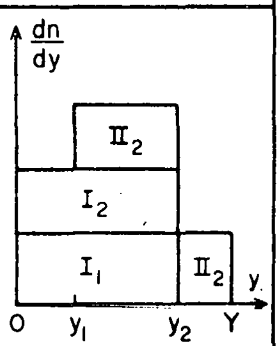

Fig. 5. pA spectra for $\bar{\nu}$ = 2.

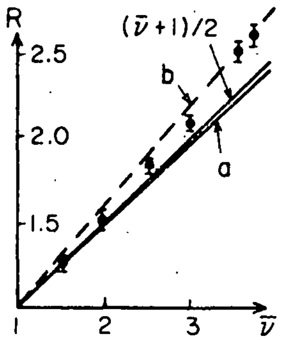

Fig. 6. $R = \langle n \rangle_{hA}/\langle n \rangle_{hh}$. See text for lines a,b.

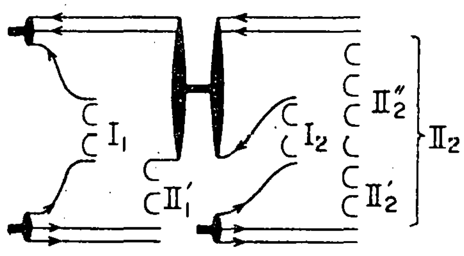

Fig. 7. pA collision for $\bar{\nu}$ = 2.

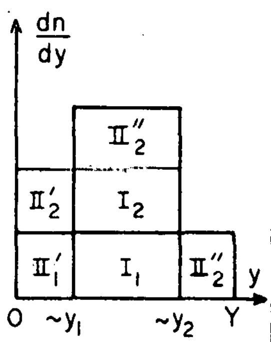

Fig. 8. pA spectra for $\bar{\nu}$ = 2.